

2MASS photometry and age estimation of the globular clusters in the outer halo of M31 *

Jun Ma^{1,2}

¹ National Astronomical Observatories, Chinese Academy of Sciences, Beijing 100012, China

² Key Laboratory of Optical Astronomy, National Astronomical Observatories, Chinese Academy of Sciences, Beijing 100012, China; majun@nao.cas.cn

Received 2011 August 22; accepted 2011 October 9

Abstract We present the first photometric results in J , H and K_s from 2MASS (Two Micron All Sky Survey) imaging of 10 classical globular clusters (GCs) in the far outer regions of M31. Combined with the V and I photometric data from previous literature, we constructed a color-color diagram between $J - K_s$ and $V - I$. By comparing the integrated photometric measurements with evolutionary models, we estimate the ages of these clusters. The results showed that all of these clusters are older than 3×10^9 yr, and among them four are older than 10 Gyr and the other six have intermediate ages between 3 – 8 Gyr. The masses for these outer-halo GCs are from $7.0 \times 10^4 M_\odot$ to $1.02 \times 10^6 M_\odot$. We argued that GC2 and GC3, whose ages, metallicities and distance moduli are almost the same, were accreted from the same satellite galaxy, if they did not form *in situ*. The statistical results show that the ages and metallicities of these 10 M31 outer-halo GCs do not vary with projected radial position, and a relationship between age and metallicity does not exist.

Key words: galaxies: halos — galaxies: individual (M31) — star clusters: general

1 INTRODUCTION

Within the popular Λ cold dark matter model for galaxy formation, substructure is expected to be seen in the outer regions of the galaxies as they continue to grow from the accretion and tidal disruption of satellite companions. Globular clusters (GCs), as luminous compact objects that are found out to distant radii in the haloes of massive galaxies, can serve as excellent tracers of substructures in the outer region of their parent galaxy. In addition, clusters, which are located at large projected distances from the center of the galaxy, provide the maximum “leverage” to constrain the mass distribution of the galaxy (see Federici et al. 1993; Evans et al. 2003; Galleti et al. 2005, and references therein). So, detailed studies on GCs in the outer halos of massive galaxies are very important.

M31, with a distance modulus of 24.47 (Holland 1998; Stanek & Garnavich 1998; McConnachie et al. 2005), is an ideal local galaxy for studying GCs since it is so near, and contains more GCs than all other Local Group galaxies combined (Battistini et al. 1987; Racine 1991; Harris 1991; Fusi Pecci et al. 1993). The globular cluster system of M31 has been the subject of intense investigations since the beginning of extragalactic astronomy (Hubble 1932). The first catalog of 140 GC candidates in

* Supported by the National Natural Science Foundation of China.

M31 was presented by Hubble (1932). From then on, numerous lists of M31 GC candidates were published. The most comprehensive catalog of GC candidates may be the Bologna catalog (Battistini et al. 1980, 1987, 1993). The Bologna catalog contains a total of 827 objects, and all the objects were classified into five classes by the authors' degree of confidence. Of these candidates, 353 were considered as class A or class B, with a high level of confidence, and the others fell into classes C, D or E. The V magnitude and $B - V$ color values for most of the candidates were presented in the Bologna catalog. Recent works have searched for fainter GCs in M31 (e.g. Mochejska et al. 1998; Barmby & Huchra 2001; Kim et al. 2007). In addition, a number of papers by Ma's group have been published on the M31 globular clusters (Fan et al. 2006, 2008, 2009; Jiang et al. 2003; Ma et al. 2006a,b, 2007, 2009b,a, 2010, 2011; Ma 2011; Wang et al. 2010), including the integrated magnitudes, colors, ages, masses, metallicities and structural parameters.

M31 GC B514 (B for "Bologna," see Battistini et al. 1987), called GC 4 in Mackey et al. (2007), is the first known outer halo cluster in M31, which is located at a projected distance of $R_p \simeq 55$ kpc. It was detected by Galletti et al. (2005) based on the XSC sources of the All Sky Data Release of the Two Micron All Sky Survey (2MASS, Cutri et al. 2003) within a $\sim 9^\circ \times 9^\circ$ area centered on M31. Now, many new members of the M31 halo GC system, which extend to very large radii, have been discovered (e.g. Huxor et al. 2005; Mackey et al. 2006, 2007; Huxor et al. 2008; Mackey et al. 2010a).

In this paper, we will study 10 outer halo GCs of M31 from Mackey et al. (2006, 2007) based on 2MASS JHK_s photometry and photometric data in the VI bands. In Section 3 we describe the details of our approach to data reduction. In Section 4 we determine the ages and masses of these outer halo GCs by comparing observational colors with population synthesis models, and in Section 5 we present some statistical results for these halo GCs. We discuss the implications of our results and provide a summary in Section 6.

2 M31 HALO GC SAMPLE

The sample of M31 halo GCs in this paper is from Mackey et al. (2006, 2007), who estimated their metallicities, distance moduli and reddening values by fitting the Galactic GC fiducials from Brown et al. (2005) to their observed color-magnitude diagrams (CMDs) in the F606W and F814W filter bands of deep images obtained using the Advanced Camera for Surveys (ACS) on board the *Hubble Space Telescope* (*HST*). These CMDs extended ~ 3 mag below the horizontal branch. In order to study the properties of M31 halo GCs, in particular to determine their ages, the metallicities and reddening values should be determined confidently. In addition, V and I photometries are needed to construct the color-color diagram (see Section 4 for details). Until now, only these 10 halo GCs have satisfied these conditions. So, the M31 halo GCs which are selected here are not a complete sample. Figure 1 shows the spatial distribution of the 10 halo GCs in M31. The large ellipse is the D_{25} boundary of the M31 disk (de Vaucouleurs et al. 1991).

3 DATA REDUCTIONS

2MASS imaged the entire sky in the near-infrared bands, J (1.2 μm), H (1.6 μm) and K_s (2.2 μm) down to a limiting sensitivity of 21.6, 20.6 and 20.0 mag arcsec $^{-2}$ (1σ), respectively, with a typical angular resolution of $\sim 2'' - 3''$ (with $1''$ pixels). For these 10 M31 halo GCs, near-infrared images in the J , H and K_s bands were extracted from the 2MASS second data release (Cutri et al. 2000) according to the coordinates presented by Mackey et al. (2006, 2007). In our analysis, the uncompressed atlas images provided by this data release were used. The pixel size of all of the 2MASS images was $1''$. An exposure time of 1.3 seconds per frame, multiplying by six frames per source, makes the total exposure 7.8 s.

Figure 2 shows the images of the 10 sample GCs observed in the J , H and K_s filters of 2MASS. The image size is $80.0'' \times 80.0''$ for each panel.

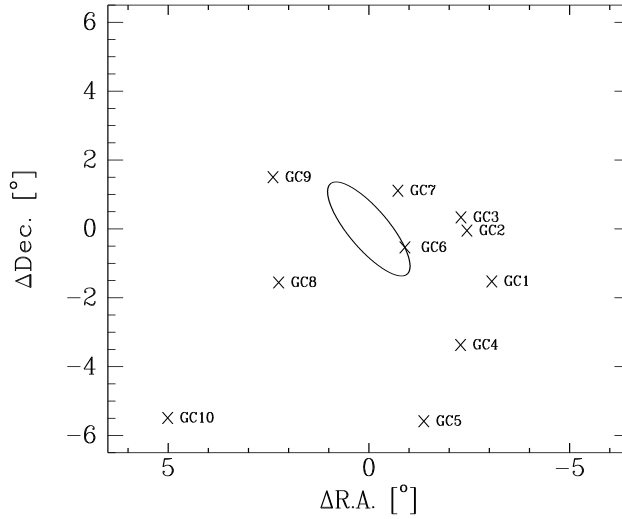


Fig. 1 Spatial distribution of the 10 M31 halo GCs. The ellipse is the D_{25} boundary of the M31 disk (de Vaucouleurs et al. 1991).

Table 1 Photometry in 2MASS J , H and K_s for 10 Halo Globular Clusters in M31

Identifier	J (mag)	H (mag)	K_s (mag)	r_{ap} ($''$)
GC1	14.116 ± 0.061	13.497 ± 0.062	13.729 ± 0.158	13.0
GC2	15.284 ± 0.106	14.419 ± 0.096	14.564 ± 0.156	9.0
GC3	14.486 ± 0.071	14.404 ± 0.101	13.904 ± 0.093	9.0
GC4	14.229 ± 0.065	13.318 ± 0.055	13.627 ± 0.098	13.0
GC5	14.314 ± 0.058	13.947 ± 0.070	13.425 ± 0.069	9.0
GC6	14.797 ± 0.076	14.495 ± 0.103	13.800 ± 0.090	13.0
GC7	16.322 ± 0.158	15.685 ± 0.199	14.861 ± 0.138	9.0
GC8	14.741 ± 0.084	13.941 ± 0.111	14.199 ± 0.155	13.0
GC9	16.723 ± 0.308	15.293 ± 0.199	15.373 ± 0.277	9.0
GC10	14.583 ± 0.076	14.268 ± 0.121	13.887 ± 0.124	13.0

We determined the magnitudes of these GCs using a standard aperture photometry approach, i.e. the PHOT routine in DAOPHOT (Stetson 1987). The relevant zero points for photometry can be obtained from the photometric header keywords of the images. These clusters lie in the halo of M31, and extraneous field stars do not exist. So accurate photometry can easily be derived. We use eight different aperture sizes (with radii of $r_{\text{ap}} = 3.0, 4.0, 5.0, 6.0, 7.0, 8.0, 9.0, 10.0, 11.0, 12.0, 13.0$ and $14.0''$) to ensure that we adopt the most appropriate photometric radius that includes all light from the objects. We decided on the size of the aperture needed for the photometry based on visual examination. The proper radius is listed in column (5) of Table 1. For $r_{\text{ap}} = 9.0''$, we adopted annuli for background subtraction spanning $10.0''$ to $15.0''$, and for $r_{\text{ap}} = 13.0''$, we adopted annuli for background subtraction spanning $14.0''$ to $19.0''$. The calibrated photometry of these objects in J , H and K_s filters is summarized in Table 1, in conjunction with the 1σ magnitude uncertainties obtained from DAOPHOT.

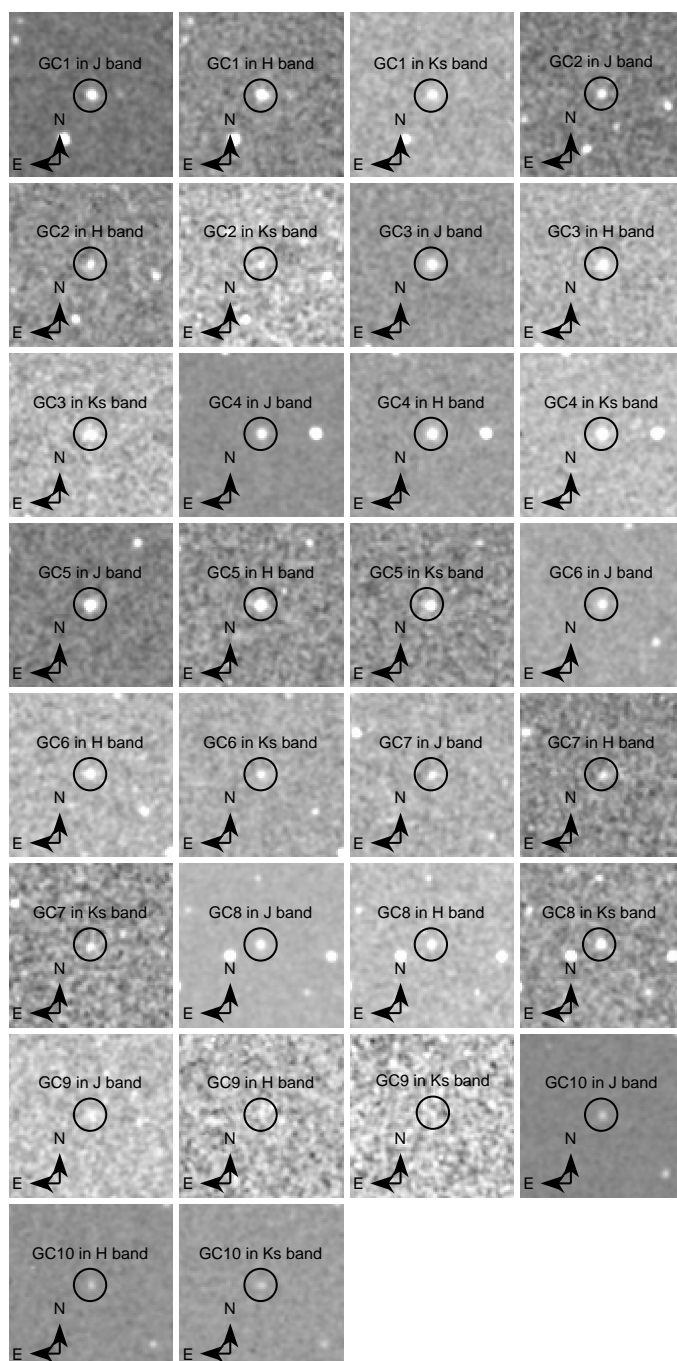


Fig. 2 Images of the 10 sample GCs observed in the J , H and K_s filters of 2MASS. The image size is $80.0'' \times 80.0''$ for each panel.

4 CLUSTER AGES AND MASSES

To determine the ages of these halo GCs, the colors to use are $(V - I)_0$ and $(J - K_s)_0$, since $(V - I)_0$ varies strongly with age when metallicity is fixed for older than 1 Gyr (see Fig. 3 below). The metallicities of our sample clusters are all determined by Mackey et al. (2006, 2007) based on the CMDs constructed using the deep images obtained by the ACS/HST. These metallicities are $-2.14 \leq [\text{Fe}/\text{H}] \leq -0.70$, which are listed in Table 2, and most of the clusters are very metal-poor. So, we use the Simple Stellar Population (SSP) models of Bruzual & Charlot (2003) (hereafter the BC03 models), which have been upgraded from the earlier Bruzual A. & Charlot (1993); Bruzual & Charlot (1996) versions, and now provide the evolution of the spectra and photometric properties for a wider range of stellar metallicities. The BC03 SSP models based on the Padova-1994 evolutionary tracks include six initial metallicities, $Z = 0.0001, 0.0004, 0.004, 0.008, 0.02 (Z_\odot)$ and 0.05, corresponding to $[\text{Fe}/\text{H}] = -2.25, -1.65, -0.64, -0.33, +0.09$ and $+0.56$, respectively. BC03 provide 26 SSP models (with both high and low spectral resolution) using the Padova-1994 evolutionary tracks, half of which were computed based on the Salpeter (1955) IMF with lower and upper-mass cut-offs of $m_L = 0.1 M_\odot$ and $m_U = 100 M_\odot$, respectively. The other 13 were computed using the Chabrier (2003) IMF with the same mass cut-offs. In addition, BC03 provide 26 SSP models using the Padova-2000 evolutionary tracks, including six partially different initial metallicities, $Z = 0.0004, 0.001, 0.004, 0.008, 0.019 (Z_\odot)$ and 0.03, i.e. $[\text{Fe}/\text{H}] = -1.65, -1.25, -0.64, -0.33, +0.07$ and $+0.29$, respectively. In this paper, we will adopt the high-resolution SSP models using the Padova-1994 evolutionary tracks and a Salpeter (1955) IMF to determine the most appropriate ages for these halo GCs, since their metallicities are $-2.14 \leq [\text{Fe}/\text{H}] \leq -0.70$ corresponding to $0.0001 \leq [\text{Fe}/\text{H}] \leq 0.004$ of the BC03 models. These SSP models contain 221 spectra describing the spectral evolution of SSPs from 1.0×10^5 yr to 20 Gyr. The evolving spectra include the contribution of the stellar components at wavelengths from 91 Å to 160 μm. BC03 include the magnitudes in the V, I and 2MASS bands, making it possible to directly obtain the colors concerned.

Table 2 Age Estimates for 10 Halo Globular Clusters in M31

Identifier	$V - I$ (mag)	$J - K_s$ (mag)	$E(B - V)$ (mag)	$(V - I)_0$ (mag)	$(J - K_s)_0$ (mag)	Metallicity (dex)	Age [log yr]
GC1	0.98 ± 0.03	0.387 ± 0.17	0.09 ± 0.01	0.83 ± 0.03	0.34 ± 0.17	-2.14	9.7 ± 0.1
GC2	0.94 ± 0.03	0.720 ± 0.19	0.08 ± 0.01	0.81 ± 0.03	0.68 ± 0.19	-1.94	9.7 ± 0.1
GC3	0.95 ± 0.03	0.582 ± 0.12	0.11 ± 0.01	0.77 ± 0.03	0.52 ± 0.12	-2.14	9.5 ± 0.2
GC4	1.08 ± 0.03	0.602 ± 0.12	0.09 ± 0.01	0.93 ± 0.03	0.56 ± 0.12	-2.14	10.2 ± 0.1
GC5	1.08 ± 0.03	0.889 ± 0.09	0.08 ± 0.01	0.95 ± 0.03	0.85 ± 0.09	-1.84	10.3 ± 0.1
GC6	1.13 ± 0.03	0.997 ± 0.12	0.09 ± 0.01	0.98 ± 0.03	0.95 ± 0.12	-2.14	10.3 ± 0.1
GC7	1.20 ± 0.03	1.461 ± 0.21	0.06 ± 0.01	1.10 ± 0.03	1.43 ± 0.21	-0.70	10.0 ± 0.1
GC8	1.04 ± 0.03	0.542 ± 0.18	0.09 ± 0.01	0.89 ± 0.03	0.50 ± 0.18	-1.54	9.9 ± 0.2
GC9	1.07 ± 0.03	1.350 ± 0.41	0.15 ± 0.01	0.83 ± 0.03	1.27 ± 0.41	-1.54	9.6 ± 0.1
GC10	0.91 ± 0.03	0.696 ± 0.15	0.09 ± 0.01	0.76 ± 0.03	0.65 ± 0.15	-2.14	9.5 ± 0.1

In Figure 3, we present the $(J - K_s)_0$ versus $(V - I)_0$ color-color diagram for the cluster samples in this paper. Overplotted with the lines are the colors for the BC03 single generation models for three metallicities, $Z = 0.004, Y = 0.2400, Z = 0.0004, Y = 0.2310$ and $Z = 0.0001, Y = 0.2303$. The age range is from 1 to 20 Gyr. The colors of $(V - I)$ are from Huxor et al. (2008), except for GC6, for which the color of $(V - I)$ is from the RBC v.4.0 (Galleti et al. 2004, 2006, 2007) since Huxor et al. (2008) did not present it. The error bars of $(V - I)$ are the photometric uncertainties, which are estimated to be ~ 0.03 mag like Huxor et al. (2008) presented, except for GC6. For GC6, which is also called B298, the magnitudes in the V and I bands are 16.59 and 15.46, respectively. The photometric uncertainties are adopted to be 0.05 as Galleti et al. (2004) suggested. The integrated

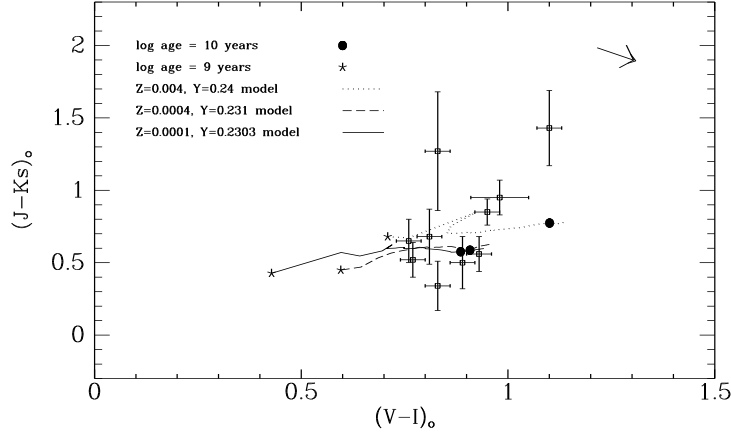


Fig. 3 $(V - I)_0$ vs. $(J - K_s)_0$ for the M31 halo GCs. The photometric errors are represented by the error bars, and the clusters have been dereddened by the reddening values from Mackey et al. (2007). The BC03 models for three separate Z values are shown. The arrow represents the direction of the reddening vector.

Table 3 Mass Estimates for 10 Halo Globular Clusters in M31

Identifier	V (mag)	$(m - M)_0$ (mag)	M/L_V $(M/L_V)_\odot$	Mass $(10^6 M_\odot)$
GC1	16.05	24.41	1.63	0.40 ± 0.07
GC2	16.98	24.32	1.63	0.15 ± 0.03
GC3	16.31	24.37	1.17	0.23 ± 0.04
GC4	15.76	24.35	3.01	0.91 ± 0.17
GC5	16.09	24.45	4.30	1.02 ± 0.19
GC6	16.59	24.49	4.30	0.69 ± 0.32
GC7	18.27	24.13	3.51	0.08 ± 0.02
GC8	16.72	24.43	2.40	0.32 ± 0.06
GC9	17.78	24.22	1.50	0.07 ± 0.01
GC10	16.50	24.42	1.21	0.20 ± 0.04

cluster colors have been dereddened by the $E(B - V)$ values given by Mackey et al. (2007). These reddening values are listed in Table 2. The interstellar extinction curve, A_λ , is taken from Cardelli et al. (1989), $R_V = A_V/E(B - V) = 3.1$. From Figure 3 we can see that the $V - I$ color is very sensitive to age when metallicity is fixed. The $J - K_s$ and $V - I$ colors of each object were compared with a model of Z that is closest to the metallicity obtained by Mackey et al. (2007) to determine the ages of the clusters. The ages obtained in this paper are listed in Table 2, and are all older than 3 Gyr. Four clusters are older than 10 Gyr, and the other six have intermediate ages between 3 – 8 Gyr.

Cluster masses can be obtained by comparing the measured luminosity in the V band with the theoretical mass-to-light (M/L) ratios. The M/L ratios are a function of the cluster age and metallicity. The mass-to-light ratios of these GCs, calculated based on the metallicity adopted and the age obtained in this paper, are listed in Table 3 for the BC03 SSP models. The magnitudes in the V band are from Huxor et al. (2008), and from the RBC v.4.0 (Galleti et al. 2004, 2006, 2007) (only for GC6). Distance moduli for these GCs are from Mackey et al. (2007). The derived masses are listed in Table 3, from which we can see that the masses of these outer halo GCs are from 7.0×10^4 to $1.02 \times 10^6 M_\odot$.

5 THE STATISTICAL PROPERTIES OF SAMPLE HALO GLOBULAR CLUSTERS

5.1 Radially Dependent Properties of Sample Halo Globular Clusters

Galactocentric coordinates for the sample halo globular clusters were computed relative to an adopted M31 central position. In this paper, we adopted a central position for M31 at $\alpha_0 = 00^{\text{h}}42^{\text{m}}44.30^{\text{s}}$ and $\delta_0 = +41^{\circ}16'09.0''$ (J2000.0) following Huchra et al. (1991) and Perrett et al. (2002). Formally,

$$X = A \sin \theta + B \cos \theta, \quad (1)$$

$$Y = -A \cos \theta + B \sin \theta, \quad (2)$$

where $A = \sin(\alpha - \alpha_0) \cos \delta$ and $B = \sin \delta \cos \delta_0 - \cos(\alpha - \alpha_0) \cos \delta \sin \delta_0$. We adopt a position angle of $\theta = 38^{\circ}$ for the major axis of M31 (Kent 1989). The X coordinate is the position along the major axis of M31, where positive X is in the northeastern direction, while the Y coordinate is along the minor axis of the M31 disk, increasing towards the northwest. The projected radius is $\sqrt{X^2 + Y^2}$.

5.1.1 Age as a function of projected distance

Gratton (1985) derived the ages of 26 Galactic GCs using the data available on the main sequence photometry, and found that as the projected galactocentric distance increases, the ages of the clusters decrease. However, this relationship in Gratton's analysis is based on the photometry for the four most distant clusters, the quality of which may not be high (see Sarajedini & King 1989, for details). Sarajedini & King (1989) calculated ages for 32 Galactic GCs using the magnitude difference between the horizontal branch and the main sequence turnoff. The statistical result showed that there was no relation between age and galactocentric distance. Subsequent work by Chaboyer et al. (1992), Sarajedini et al. (1995) and Chaboyer et al. (1996) reinforced the results of Sarajedini & King (1989) using larger and more reliable data sets of GC ages as well as a variety of techniques for measuring them. Based on the uniform photometric data set provided by the ACS/HST Galactic GC Treasury project (Sarajedini et al. 2007), Marín-Franch et al. (2009) and Dotter et al. (2010) determined the ages from a large sample of GCs. The statistical results of Marín-Franch et al. (2009) and Dotter et al. (2010) also showed that there is no relation between age and galactocentric distance. Figure 4 shows the distribution of age against projected galactocentric distance for these 10 outer halo GCs. Here we note that no relationship exists. This conclusion is consistent with Sarajedini & King (1989) and their series of works.

5.1.2 Mass as a function of projected distance

Figure 5 shows the distribution of mass against projected galactocentric distance for these 10 outer-halo GCs. However, there is no relationship between mass and galactocentric distance.

5.1.3 Metallicity as a function of projected distance

One early formation model by Eggen et al. (1962) argues for a single, large-scale collapse of material to form galactic bodies such as the Milky Way, in which the enrichment timescale is shorter than the collapse time, and so the halo stars and GCs should show large-scale metallicity gradients. A principal competing model maintains that formation occurred through random mergers of fragmented gas clouds over the course of billions of years, implying a hierarchical origin (Searle & Zinn 1978), so there should be a homogeneous metallicity distribution.

For M31 GCs, there are some inconsistent conclusions. For example, van den Bergh (1969) showed that there is little or no evidence for a correlation between metallicity and projected radius,

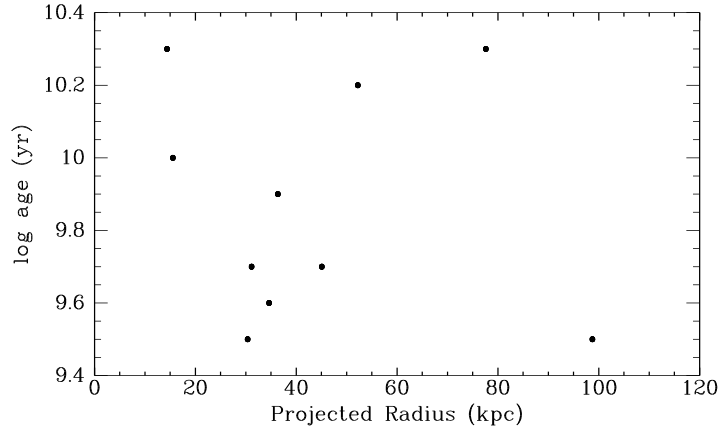


Fig. 4 Age as a function of galactocentric distance for these 10 outer-halo GCs in M31.

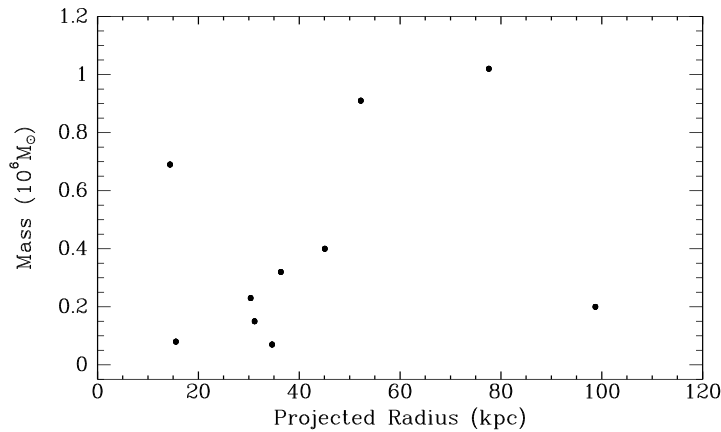


Fig. 5 Mass as a function of galactocentric distance for these 10 outer-halo GCs in M31.

but most of his clusters were inside $50''$; however, some authors (see, e.g. Huchra et al. 1982; Sharov 1988; Huchra et al. 1991) have presented evidence for a weak but measurable metallicity gradient as a function of projected radius. Barmby et al. (2000), Perrett et al. (2002) and Fan et al. (2008) confirmed the latter result based on their large sample of spectral metallicity and color-derived metallicity.

Figure 6 shows the distribution of metallicities against projected galactocentric distance for these 10 outer halo GCs. Clearly, the dominant feature of this diagram is the scatter in metallicity at any radius. However, the most distant globular cluster (GC10) is really very metal-poor. We also noted that the metallicity of GC6 is very low ($[\text{Fe}/\text{H}] = -2.14$), and the metallicity of GC7 is very high ($[\text{Fe}/\text{H}] = -0.7$). However, these two clusters lie almost the same distance from the center of M31 (see Fig. 6). This result is consistent with Yang et al. (2010)'s finding for the halo populations of M33: the halo populations show no trend of metal abundance with radial position.

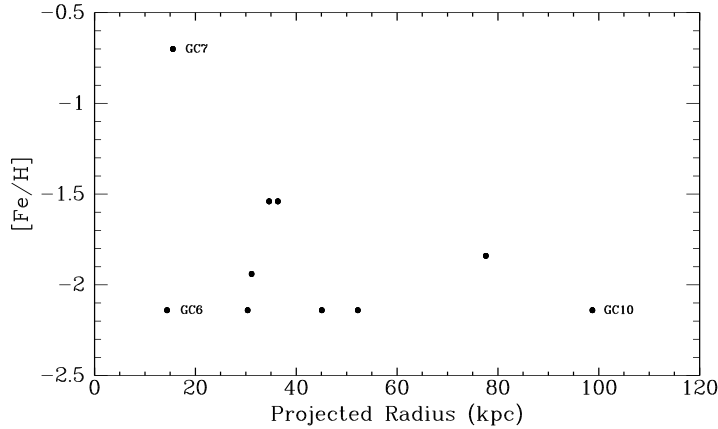


Fig. 6 Metallicity as a function of galactocentric distance for the 10 outer-halo GCs in M31.

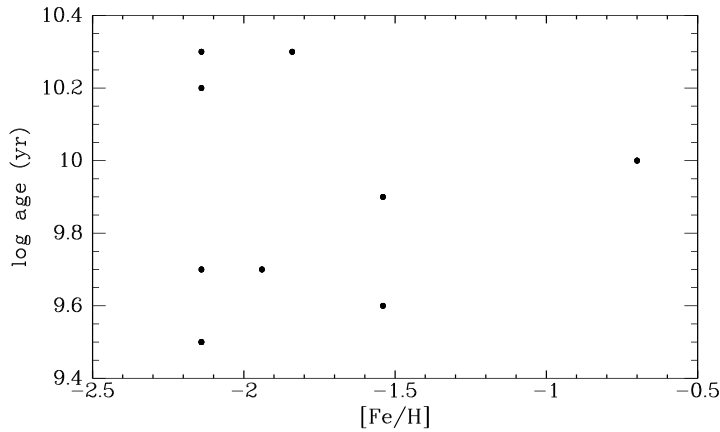


Fig. 7 Relationship between age and metallicity for the 10 outer-halo GCs in M31.

5.2 Relationship between Age and Metallicity for Sample Halo Globular Clusters

The Galactic GC system is known to obey a clear age-metallicity relationship, in the sense of older GCs being characterized by generally lower metallicities (e.g., Sarajedini & King 1989; Chaboyer et al. 1996). Fan et al. (2006) showed that although there is significant scatter in metallicity at any age, there is a notable lack of young metal-poor and old metal-rich GCs, which might be indicative of an underlying age-metallicity relationship among the M31 GC population.

Figure 7 shows the metallicity as a function of age for the outer halo GC sample discussed in this paper. It is evident that there is no relationship between age and metallicity.

5.3 Relationship between Age and Mass for Sample Halo Globular Clusters

Figure 8 shows the mass as a function of age for the outer halo GC sample discussed in this paper. It appears that a general trend between GC age and mass may exist, in the sense that more massive clusters are older, except for GC7, which has a mass of $8.0 \times 10^4 M_{\odot}$. However, its age is ~ 10 Gyr.

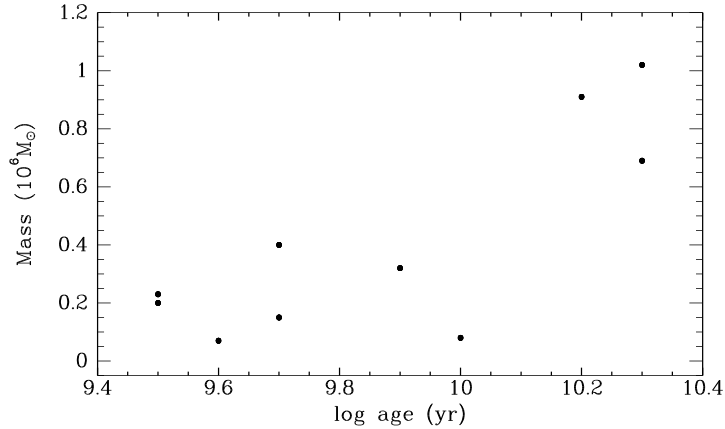


Fig. 8 Relationship between age and mass for these 10 outer-halo GCs in M31.

6 SUMMARY AND DISCUSSION

This paper firstly presented photometric results in J , H and K_s from 2MASS imaging for 10 classical GCs in the far outer regions of M31. Combined with the V and I photometric data from previous literature, we constructed the color-color diagram between $J - K_s$ and $V - I$. By comparing the integrated photometric measurements with evolutionary models, we estimated the ages of these clusters. The results showed that all of these clusters are older than 3 Gyr. In addition, we estimated the masses for these outer-halo GCs, which are from 7.0×10^4 to $1.02 \times 10^6 M_{\odot}$.

In their seminal work, Searle & Zinn (1978) examined the abundances of a sample of Galactic GCs, and found that there is no radial abundance gradient in the cluster system of the outer halo. They argued that this fact, along with a broad spread in the color distribution on the horizontal branch for distant GCs, implied that a significant fraction of GCs at Galactocentric radii ≥ 8 kpc formed in smaller “proto-galactic fragments” that were subsequently accreted into the Galactic potential well. Recent work by Marín-Franch et al. (2009), Gratton et al. (2010) and Dotter et al. (2010) showed that the Galactic GCs (with Galactocentric radii > 8 kpc) exhibit properties consistent with having been accreted in a relatively slow and chaotic fashion from dwarf satellite galaxies of the Milky Way (see also Yang et al. 2010). Based on a sample of newly discovered GCs from the Pan-Andromeda Archaeological Survey, in combination with previously cataloged objects, Mackey et al. (2010b) mapped the spatial distribution of GCs in the M31 halo. The GCs studied here are also included in the sample of Mackey et al. (2010b). Mackey et al. (2010b) found that at projected radii beyond 30 kpc, where large coherent stellar streams are readily distinguished in the field, there is a striking correlation between these features and the positions of the GCs. Using a simple Monte Carlo simulation, they computed the probability that it could be due to the chance alignment of GCs smoothly distributed in the M31 halo, and found the likelihood of this possibility is low, below 1%, which implied that the majority of the remote GC systems of M31 was accreted from satellite galaxies.

It is interesting that GC2 and GC3 have ages and metallicities that are nearly the same (the ages for GC2 and GC3 are $\log \text{age} = 9.7$ and 9.5 , respectively, and the metallicities for GC2 and GC3 are $[\text{Fe}/\text{H}] = -1.94$ and -2.14 , respectively). In addition, from Mackey et al. (2007), the distance moduli of GC1 and GC2 are $(m - M)_0 = 24.32 \pm 0.14$ and $(m - M)_0 = 24.37 \pm 0.15$ respectively, i.e. they are very close. So, we argued that GC2 and GC3 were accreted from the same satellite galaxy, if they did not form in M31.

Acknowledgements We would like to thank the referee, Professor Jingyao Hu, for providing a rapid and thoughtful report that helped improve the original manuscript greatly. This work was supported by the National Natural Science Foundation of China (Grant Nos. 10873016 and 10633020), and by the National Basic Research Program of China (973 Program, No. 2007CB815403).

References

- Barmby, P., & Huchra, J. P. 2001, *AJ*, 122, 2458
- Barmby, P., Huchra, J. P., Brodie, J. P., et al. 2000, *AJ*, 119, 727
- Battistini, P., Bonoli, F., Braccesi, A., et al. 1980, *A&AS*, 42, 357
- Battistini, P., Bonoli, F., Braccesi, A., et al. 1987, *A&AS*, 67, 447
- Battistini, P. L., Bonoli, F., Casavecchia, M., et al. 1993, *A&A*, 272, 77
- Brown, T. M., Ferguson, H. C., Smith, E., et al. 2005, *AJ*, 130, 1693
- Bruzual, A. G., & Charlot, S. 1996, unpublished
- Bruzual, G., & Charlot, S. 2003, *MNRAS*, 344, 1000
- Bruzual A., G., & Charlot, S. 1993, *ApJ*, 405, 538
- Cardelli, J. A., Clayton, G. C., & Mathis, J. S. 1989, *ApJ*, 345, 245
- Chaboyer, B., Demarque, P., & Sarajedini, A. 1996, *ApJ*, 459, 558
- Chaboyer, B., Sarajedini, A., & Demarque, P. 1992, *ApJ*, 394, 515
- Chabrier, G. 2003, *PASP*, 115, 763
- Cutri, R. M., et al. 2000, Explanatory Supplement to the 2MASS Second Incremental Data Release (Pasadena: Caltech)
- Cutri, R. M., Skrutskie, M. F., van Dyk, S., et al. 2003, 2MASS All Sky Catalog of Point Sources <http://www.ipac.caltech.edu/2mass/release/allsky/doc/explsup.html>
- de Vaucouleurs, G., de Vaucouleurs, A., Corwin, H. G., Jr., et al. 1991, *Third Reference Catalogue of Bright Galaxies* (New York: Springer), 548
- Dotter, A., Sarajedini, A., Anderson, J., et al. 2010, *ApJ*, 708, 698
- Eggen, O. J., Lynden-Bell, D., & Sandage, A. R. 1962, *ApJ*, 136, 748
- Evans, N. W., Wilkinson, M. I., Perrett, K. M., & Bridges, T. J. 2003, *ApJ*, 583, 752
- Fan, Z., Ma, J., de Grijs, R., Yang, Y., & Zhou, X. 2006, *MNRAS*, 371, 1648
- Fan, Z., Ma, J., de Grijs, R., & Zhou, X. 2008, *MNRAS*, 385, 1973
- Fan, Z., Ma, J., & Zhou, X. 2009, *RAA* (Research in Astronomy and Astrophysics), 9, 993
- Federici, L., Bonoli, F., Ciotti, L., et al. 1993, *A&A*, 274, 87
- Fusi Pecci, F., Cacciari, C., Federici, L., & Pasquali, A. 1993, in *ASPC Series 48, The Globular Cluster-Galaxy Connection*, eds. G. H. Smith, & J. P. Brodie, 410
- Galletti, S., Bellazzini, M., Federici, L., Buzzoni, A., & Fusi Pecci, F. 2007, *A&A*, 471, 127
- Galletti, S., Bellazzini, M., Federici, L., & Fusi Pecci, F. 2005, *A&A*, 436, 535
- Galletti, S., Federici, L., Bellazzini, M., Buzzoni, A., & Fusi Pecci, F. 2006, *ApJ*, 650, L107
- Galletti, S., Federici, L., Bellazzini, M., Fusi Pecci, F., & Macrina, S. 2004, *A&A*, 416, 917
- Gratton, R. G. 1985, *A&A*, 147, 169
- Gratton, R. G., Carretta, E., Bragaglia, A., Lucatello, S., & D'Orazi, V. 2010, *A&A*, 517, A81
- Harris, W. E. 1991, *ARA&A*, 29, 543
- Holland, S. 1998, *AJ*, 115, 1916
- Hubble, E. 1932, *ApJ*, 76, 44
- Huchra, J., Stauffer, J., & van Speybroeck, L. 1982, *ApJ*, 259, L57
- Huchra, J. P., Brodie, J. P., & Kent, S. M. 1991, *ApJ*, 370, 495
- Huxor, A. P., Tanvir, N. R., Ferguson, A. M. N., et al. 2008, *MNRAS*, 385, 1989
- Huxor, A. P., Tanvir, N. R., Irwin, M. J., et al. 2005, *MNRAS*, 360, 1007
- Jiang, L., Ma, J., Zhou, X., et al. 2003, *AJ*, 125, 727

- Kent, S. M. 1989, *AJ*, 97, 1614
- Kim, S. C., Lee, M. G., Geisler, D., et al. 2007, *AJ*, 134, 706
- Ma, J. 2011, *RAA (Research in Astronomy and Astrophysics)*, 11, 524
- Ma, J., de Grijs, R., Fan, Z., et al. 2009a, *RAA (Research in Astronomy and Astrophysics)*, 9, 641
- Ma, J., de Grijs, R., Yang, Y., et al. 2006a, *MNRAS*, 368, 1443
- Ma, J., Fan, Z., de Grijs, R., et al. 2009b, *AJ*, 137, 4884
- Ma, J., van den Bergh, S., Wu, H., et al. 2006b, *ApJ*, 636, L93
- Ma, J., Wang, S., Wu, Z., et al. 2011, *AJ*, 141, 86
- Ma, J., Wu, Z., Wang, S., et al. 2010, *PASP*, 122, 1164
- Ma, J., Yang, Y., Burstein, D., et al. 2007, *ApJ*, 659, 359
- Mackey, A. D., Ferguson, A. M. N., Irwin, M. J., et al. 2010a, *MNRAS*, 401, 533
- Mackey, A. D., Huxor, A., Ferguson, A. M. N., et al. 2006, *ApJ*, 653, L105
- Mackey, A. D., Huxor, A., Ferguson, A. M. N., et al. 2007, *ApJ*, 655, L85
- Mackey, A. D., Huxor, A. P., Ferguson, A. M. N., et al. 2010b, *ApJ*, 717, L11
- Marín-Franch, A., Aparicio, A., Piotto, G., et al. 2009, *ApJ*, 694, 1498
- McConnachie, A. W., Irwin, M. J., Ferguson, A. M. N., et al. 2005, *MNRAS*, 356, 979
- Mochejska, B. J., Kaluzny, J., Krockenberger, M., Sasselov, D. D., & Stanek, K. Z. 1998, *Acta Astronomica*, 48, 455
- Perrett, K. M., Bridges, T. J., Hanes, D. A., et al. 2002, *AJ*, 123, 2490
- Racine, R. 1991, *AJ*, 101, 865
- Salpeter, E. E. 1955, *ApJ*, 121, 161
- Sarajedini, A., Bedin, L. R., Chaboyer, B., et al. 2007, *AJ*, 133, 1658
- Sarajedini, A., & King, C. R. 1989, *AJ*, 98, 1624
- Sarajedini, A., Lee, Y.-W., & Lee, D.-H. 1995, *ApJ*, 450, 712
- Searle, L., & Zinn, R. 1978, *ApJ*, 225, 357
- Sharov, A. S. 1988, *Soviet Astronomy Letters*, 14, 339
- Stanek, K. Z., & Garnavich, P. M. 1998, *ApJ*, 503, L131
- Stetson, P. B. 1987, *PASP*, 99, 191
- van den Bergh, S. 1969, *ApJS*, 19, 145
- Wang, S., Fan, Z., Ma, J., de Grijs, R., & Zhou, X. 2010, *AJ*, 139, 1438
- Yang, S.-C., Sarajedini, A., Holtzman, J. A., & Garnett, D. R. 2010, *ApJ*, 724, 799